Unique Ligand−Protein Interactions in a New Truncated Hemoglobin from *Mycobacterium tuberculosis*†

Masahiro Mukai,‡ Pierre-Yves Savard,§ Hugues Ouellet,§ Michel Guertin,§ and Syun-Ru Yeh*,‡

Department of Physiology and Biophysics, Albert Einstein College of Medicine, Bronx, New York 10461, and Department of Biochemistry and Microbiology, Faculty of Sciences and Engineering, Laval University, Quebec G1K 7P4, Canada

Received August 3, 2001; Revised Manuscript Received January 15, 2002

ABSTRACT: A new truncated hemoglobin (HbO) from *Mycobacterium tuberculosis* has been expressed and purified. Sequence alignment of HbO with other hemoglobins suggests that the proximal F8 residue is histidine and the distal E7 and the B10 positions are occupied by alanine and tyrosine, respectively. The highly conserved residue at the CD1 position, surprisingly, is tyrosine, making HbO the first exception in the hemoglobin family that does not contain phenylalanine at this position. Resonance Raman data suggest that a strong hydrogen bonding network, involving the B10 Tyr and the CD1 Tyr, stabilizes the heme-bound O_2 and CO as evidenced by the relatively low frequency of the Fe−O_2 stretching mode (559 cm^{-1}) and the high frequency of the Fe−CO stretching mode (527 cm^{-1}). The presence of this hydrogen bonding network is supported by mutagenesis studies with the B10 tyrosine or the CD1 tyrosine mutated to phenylalanine. Taken together, these data demonstrate a rigid and polar distal pocket in HbO, which is significantly different from that of HbN, the other hemoglobin from *M. tuberculosis*. The distinct features in the heme active site structures and the temporal expression patterns of HbO and HbN suggest that these two hemoglobins may have very different physiological functions.

Recent discoveries of hemoglobins in unicellular organisms (*1*−*7*) introduce a new twist to the common perception that hemoglobin is an oxygen carrier, in view of the fact that oxygen delivery is a diffusion-controlled process in these cells. On the basis of sequence alignments, two groups of hemoglobins have been identified in unicellular organisms (*4*, *8*−*12*). The first group consists of flavohemoglobins from bacteria and fungi (*13*−*17*). Members of this group contain a heme domain with a classical three-over-three α-helical sandwich motif (*14*), and a flavin-containing reductase domain either covalently or noncovalently associated with the heme domain (*18*, *19*). The second group consists of small Hbs with a novel two-over-two α-helical sandwich motif (*4*, *20*, *21*). They have been termed truncated hemoglobins (trHbs)[1] and are characterized by the absence of the A-helix and the presence of an extended loop substituting for most of the F-helix (*4*).

Two genes, *glbN* and *glbO*, encoding trHbs (HbN and HbO, respectively) were recently discovered in the complete genome sequence of the virulent *Mycobacterium tuberculosis* (*22*). The extent of amino acid identity between the two proteins is only 18%. Structure-based sequence alignment (Figure 1) suggests that the structural fingerprint for trHbs, including the presence of three glycine motifs and the occupancy of the B9 and E14 positions by two Phe residues (*4*), is present in both HbN and HbO. In HbN, the proximal ligand to the heme is His and the distal residues at the E7 and B10 positions, which stabilize heme-bound ligands in other hemoglobins (*12*, *23*−*26*), are Leu and Tyr, respectively. In HbO, the proximal ligand to the heme is also His and the distal residues at the E7 and B10 positions are Ala and Tyr, respectively. More interestingly, the highly conserved CD1 residue, which is Phe in all hemoglobins studied to date, is Tyr in HbO. HbO thus represents the first example of native Hb that does not have Phe at the CD1 position. It is important to point out that some of the naturally occurring human Hb mutants do not have Phe at the CD1 position (*27*). In addition, a Tyr residue is found in the CD1 position of other putative trHbs from *Mycobacterium leprae*, *Mycobacterium avium*, *Cornybacterium diphterae*, and *Streptomyces coelicolor* (Figure 1) (*21*).

In previous reports, we demonstrated that the B10 Tyr in HbN donates a strong hydrogen bond to the heme-bound dioxygen (*28*, *29*). We proposed that an important function of HbN is to protect *M. tuberculosis* against reactive nitrogen species and the unique hydrogen bonding network between the B10 Tyr and the dioxygen activates the O−O bond and thereby facilitates its reaction with NO to produce nitrate (*28*, *29*). On the other hand, the physiological function of HbO is totally unexplored. The presence of two trHbs in *M. tuberculosis*, like the multiple copies of β-globin genes in mammals (*30*), may originate from a gene duplication event. Gene duplication events can produce proteins with redundant functions, which might insulate an organism against otherwise deleterious mutations (*31*). They can also produce proteins with diverged functions, which might promote functional diversification and biochemical innovation through mutations and recombination of duplicates (*31*). In an effort

† This work was supported by National Institutes of Health Grant HL65465 to S.-R.Y. and Natural Sciences and Engineering Research Council of Canada Grant 06P0046306 to M.G.

* To whom correspondence should be addressed. Telephone: (718) 430-4234. Fax: (718) 430-4230. E-mail: syeh@aecom.yu.edu.

‡ Albert Einstein College of Medicine.

§ Laval University.

[1] Abbreviations: trHb, truncated hemoglobin; BCG, *Bacillus* Calmette-Gue′rin; Hb, hemoglobin; Mb, myoglobin.

10.1021/bi0156409 CCC: $22.00
Published on Web 02/27/2002

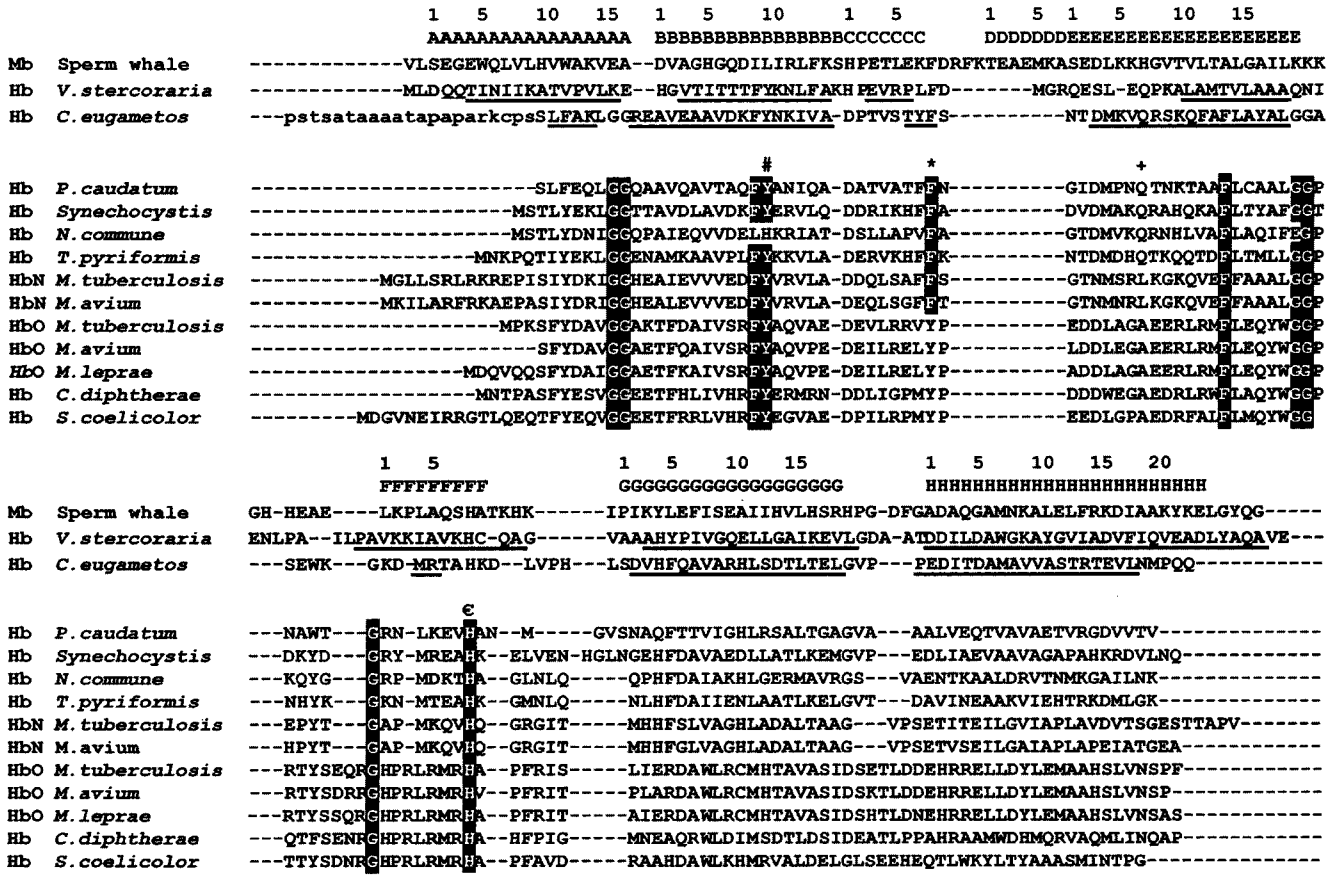

FIGURE 1: Structure-based sequence alignment of *M. tuberculosis* HbO and of 11 trHbs from different sources. The sequences of sperm whale (*Physeter catodon*) Mb, *Vitreoscilla* sp. Hb, and *C. eugametos* trHb are taken as references for vertebrate globins, bacterial Hbs, and bacterial trHbs, respectively. The topological positions for the globin fold, as defined in sperm whale Mb, are shown on the top of the aligned sequences. Helices in *C. eugametos* Hb and *Vitreoscilla* sp. Hb are underlined. Sequence accession numbers: X72919 for *C. eugametos* Hb, P15160 for *Physeter caudatum*, D90910 for *Synechocystis* PCC6803 Hb, L47979 for *Nostoc commune* Hb, P17724 for *Tetrahymenis pyriformis* Hb, Z74020 for *M. tuberculosis* HbN, AL021246 for *M. tuberculosis* HbO, CAC31634 for *M. leprae* HbO, and CAB71209 for *S. coelicolor* HbO. Preliminary sequence data for *M. avium* (HbN and HbO) were obtained from The Institute for Genomic Research. Sequence data for *Chlamydomonas diphterae* were produced by the Sequencing Group at the Sanger Center and can be obtained from ftp://ftp.sanger.ac.uk/pub/pathogens/cj and ftp://ftp.sanger.ac.uk/pub/pathogens/bp. Important residues with regard to coordination of the heme and the ligand binding residues properties are indicated: (#) tyrosine at B10, (*) phenylalanine at CD1, (+) distal position at E7, and (crossed C) proximal histidine at F8. Glycine motifs that contribute to the achievement of the trHb fold and the highly conserved Phe at B9 and E14 are also shown in reverse type.

to facilitate the understanding of the physiological functions of HbN and HbO, we followed the temporal expression pattern of HbO with Western blot analysis, in comparison with HbN, during the growth cycle of *Mycobacterium bovis* BCG cells (a model system for *M. tuberculosis*). In addition, we used resonance Raman spectroscopy, combined with site-directed mutagenesis, to investigate the structural and functional properties of HbO. The peculiar distal heme pocket structure of HbO is discussed in detail and is compared to that of HbN.

EXPERIMENTAL PROCEDURES

Bacterial Strains and Culture Conditions. *M. bovis* BCG ATCC 35734 cells were grown at 37 °C with constant shaking at 150 rpm in 300 mL Nephelo flasks containing 150 mL of 7H9 medium supplemented with 15 mL of Middlebrook ADC enrichment medium, 0.6% glycerol, and 0.05% Tween-80. ADC contains 5% bovine serum albumin fraction V, 2% glucose, and 0.85% NaCl.

Cloning, Expression, and Purification of Recombinant HbO. We used the polymerase chain reaction to amplify the coding region of the *glbO* gene from *M. bovis* BCG ATCC 35734 genomic DNA. The DNA primers that were used were 5′ GCTGTTCCATATGCCGAAGTCTTTCTACGACG 3′ (upper primer) and 5′ CGGGATCCTCAAAACGGGGAGTTGACCAGCG 3′ (lower primer). The *Nde*I−*Bam*HI-digested PCR fragment was cloned into the pET-3A prokaryotic expression vector, and the recombinant protein was expressed in freshly transformed *Escherichia coli* BL21-(DE3) cells. The amino acid sequence of BCG ATCC 35734 HbO was found to be 100% identical to that of *M. tuberculosis* H37Rv. The sequence has been deposited at National Center for Biotechnology Information data bank (accession number AF213450).

Cells were grown at 37 °C in 2 L flasks containing 850 mL of Luria-Bertani medium and 200 μg/mL ampicilin until the absorption at 600 nm reached 0.5−0.8, at which point they were incubated for an additional 2 h. The cells were harvested by centrifugation at 5000*g* for 15 min at 4 °C, resuspended in 0.02 volume of buffer containing 50 mM Tris-HCl (pH 7.5), 50 μM EDTA, and 1 mM phenylmethanesulfonyl fluoride, and disrupted by passing them twice through a French pressure cell operated at 20 000 psi (cooled at 4 °C). Cell debris was removed by centrifugation

at 12000*g* for 30 min at 4 °C. The extract was then fractionated with ammonium sulfate (40−80% saturation). The precipitate was collected by centrifugation at 10000*g* for 20 min, resuspended in 10 mM Tris-HCl (pH 8) and 50 μM EDTA, and dialyzed against the same buffer overnight at 4 °C in 6−8 kDa molecular mass cutoff membranes from Spectrapor.

The dialysate was then loaded onto a XK 26/40 column of DEAE-Sepharose Fast-Flow (135 mL) (Pharmacia), equilibrated with 10 mM Tris-HCl (pH 8) and 50 μM EDTA at 4 °C. The column was washed with 10 mM Tris-HCl (pH 8), 50 μM EDTA, and 50 mM NaCl until the absorption at 280 nm was less than 0.05. The protein was eluted with a linear gradient (1350 mL) of 50 to 150 mM NaCl. Fractions with a 410 nm/280 nm ratio of >0.8 were pooled and concentrated by ammonium sulfate precipitation (95% saturation). The protein was then resuspended in 1−2 mL of buffer containing 50 mM Tris-HCl (pH 7.5), 50 μM EDTA, and 300 mM NaCl, dialyzed against the same buffer overnight at 4 °C, and passed through a HiLoad 16/60 Superdex 75 gel-filtration column (prep grade, Pharmacia) equilibrated with the same buffer at 4 °C. Fractions with a 410 nm/280 nm ratio of >2.4 were pooled and concentrated by ammonium sulfate precipitation, as described previously, and were dialyzed against 10 mM Tris-HCl (pH 8) and 50 μM EDTA overnight at 4 °C. The protein was then loaded onto a Resource Q 6 mL column (Pharmacia) and eluted with a linear gradient (120 mL) of 0 to 200 mM NaCl in 10 mM Tris-HCl (pH 8) and 50 μM EDTA at 4 °C. Fractions with a 410 nm/280 nm ratio of >3.0 were pooled and concentrated by ammonium sulfate precipitation, as described previously, and were dialyzed against 50 mM Tris-HCl (pH 7.5) and 50 μM EDTA overnight at 4 °C. Protein purity was assessed by SDS−PAGE. The heme was identified and quantified by the pyridine−hemochrome method (*32*). Using this procedure, 1.0−1.2 mg of highly purified protein was obtained per liter of growth medium.

Western Blot Analysis. Polyclonal antibodies against HbO were obtained as described previously (*11*) except that Titermax (CytRx Corp.) was used in place of Freund's adjuvant. Western blot analysis was performed as previously described (*11*). It was obtained by probing the membrane first with trHbN antibodies and then with trHbO antibodies. Identical results were obtained by probing first with trHbO antibodies. We also stained the membrane after the immunodetection procedure to ensure equal loading in the different wells.

Optical Absorption Spectroscopy. Optical absorption spectra were recorded using a Cary model 3E spectrophotometer (Varian) equipped with a temperature-controlled multicell holder. Ferric samples were prepared at room temperature by oxidation of the oxy form, purified from *E. coli* cells, with a 10-fold excess of potassium ferricyanide. After the reaction was allowed to proceed to completion, the protein was purified from the ferri/ferrocyanide by desalting over a P6DG column equilibrated with 10 mM Tris-HCl buffer (pH 7.5) containing 50 μM EDTA. Oxy samples were prepared either from the ferric protein with an enzymatic reducing system or by exposing to air the ligand-free ferrous Hb prepared in an anaerobic chamber (Labmaster 100, MBraun). CO samples were prepared by first incubating anaerobically the Hb with CO followed by reduction with sodium dithionite. All spectra were recorded at room temperature.

Site-Directed Mutagenesis. The single-amino acid substitution mutants of HbO (B10 Tyr → Phe and CD1 Tyr → Phe) were prepared as described previously (*28*).

Resonance Raman Spectroscopy. The Raman measurements were taken with previously described instrumentation (*29*). The protein was buffered at the desired pH with 50 mM Tris and CAPS buffers at pH 7.5 and 10.5, respectively. For all of the experiments reported here, the protein concentration was 50 μM. The oxy and CO derivatives were prepared by exposing the dithionite-reduced protein to either air or CO in tightly sealed Raman cells. With this method, a small amount of ferric form was always present in the oxy sample; however, the spectral contribution from the ferric protein was canceled out in the isotope difference spectra. Optical absorption spectra were obtained before and after the Raman measurements to ensure the stability of the protein samples. The corresponding $^{18}O_2$- or $^{13}C^{18}O$-substituted samples were prepared with the same protocol. The output at 406.7 or 413.1 nm from a krypton ion laser (Spectra Physics) was focused to an ~30 μm spot (laser power of ~2 mW) on a rotating cell to prevent photodamage to the sample. The acquisition time was ~15 min for each spectrum. The scattered light was collected at right angles to the incident beam and focused on the entrance slit of a 1.25 m polychromator (Spex) where it was dispersed and then detected by a charge-coupled device camera (Princeton Instruments).

RESULTS

Biochemical Properties of Recombinant HbO. To demonstrate that the *glbO* gene encodes a functional trHb and to gain information about the biochemical and biophysical properties of the protein, the recombinant HbO protein was expressed in *E. coli* and purified to near homogeneity. The purified protein contained a heme and was identified as an iron−protoporphyrin IX protein from the oxidized-minus-reduced pyridine−hemochromogen spectrum (*32*). The apoprotein migrated with an apparent molecular mass of 14.9 kDa, as estimated by SDS−PAGE. This value is close to that predicted from sequence analysis of the 128-amino acid hydrophilic polypeptide (14.9 kDa).

HbO reacts reversibly with oxygen with high affinity, $p_{50} \cong 0.02$ mmHg (M. Guertin et al., unpublished data), characteristic of many trHbs (*21*). This oxygen affinity is much higher than that of sperm whale Mb (0.51 mmHg), and slightly lower than that of HbN (0.013 mmHg). In sharp contrast to the findings with *M. tuberculosis* HbN and *Chlamydomonas* trHb (*12*, *28*), mutation of the B10 tyrosine, TyrB10 → Phe, results in only a minor decrease in oxygen affinity ($p_{50} \cong 0.04$ mmHg). The lower oxygen binding affinity of HbO as compared to that of HbN, and its insensitivity to the mutation in the B10 residue, can be ascribed to its unique distal heme environment as will be discussed below.

Optical Absorption Spectra. Optical absorption spectra revealed that HbO can bind a variety of ligands. The optical absorption spectrum of the ferric species at pH 7.5 is a mixture of low- and high-spin heme ($\lambda_{max} = 409$, 540, 580, and 634 nm; Figure 2). The wavelengths for the electronic

Table 1: Frequencies of the Iron−Histidine (Fe−His), Iron−Hydroxide (Fe−OH^-), Iron−CO (Fe−CO) and Iron−O_2 (Fe−O_2) Stretching Modes of Various Heme-Containing Proteins Determined by Resonance Raman Scattering[a]

protein	ν_{Fe-His}	ν_{Fe-OH}	ν_{Fe-CO}	ν_{Fe-O_2}	ν_{O-O}	ref
HbO	226	446 (HS), 533 (LS)	525	559	1140	this work
HbO B10 Y → F	226	446 (HS), 510 (LS)	525	559	−	this work
HbO CD1 Y → F	226	510 (LS)	515	556	−	this work
HbN	226	456 (HS), 560 (LS)	500, 535	560	−	*28*, *29*
HbN B10 Y → F	226	552 (LS)	502	570	−	*28*, *29*
sperm whale Mb	220	490 (HS), 551 (LS)	507	569	−	*40*−*42*
human Hb	216	492 (HS), 553 (LS)	506	571	−	*40*−*42*
Scapharca Hb	203	578 (5C)	517	568	−	*41*, *46*
Ascaris sum Hb	206	nd	515, 543	nd	−	*26*, *47*
barley Hb	219	nd	493, 534	nd	−	*48*
Chlamydomonas Hb	232	nd	491	554	1136	*12*, *49*
Paramecium Hb	220	nd	493	563	−	*50*
Synechocystis Hb	nd	nd	492	554	1133	*49*, *51*
CCP	227, 248	nd	505, 537	nd	−	*52*
HRP	241, 244	503 (LS)	531, 541	562	−	*40*, *42*, *52*, *53*

[a] HS, LS, and 5C stand for high-spin, low-spin, and five-coordinate species, respectively. CCP and HRP are cytochrome *c* peroxidase and horseradish peroxidase, respectively. nd means not determined.

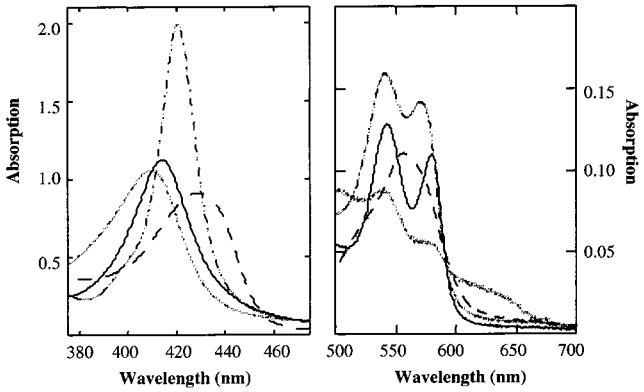

FIGURE 2: Optical absorption spectra of HbO. The absorption optical spectra of the oxy (—), ferrous (− − −), CO (—···—), and ferric (···) forms were recorded in 50 mM Tris-HCl (pH 7.5) containing 50 μM EDTA at 23 °C. The concentration of HbO is 10 μM.

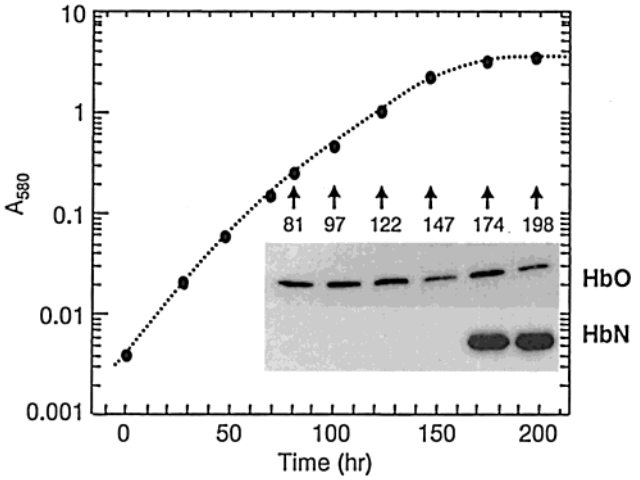

FIGURE 3: Temporal expression pattern of HbN and HbO in *M. bovis* BCG cells. BCG cells (ATCC 35734) were grown at 37 °C with constant shaking. Aliquots of suspension were taken at the indicated times for absorption determination at 580 nm and Western blot analysis of total proteins (each lane contains 5 μg of protein extract). The detection was performed using polyclonal antibodies raised against HbN and HbO.

transitions of the oxy (λ_{max} = 414, 543, and 580 nm; Figure 2) and carbon monoxide (λ_{max} = 420, 541, and 571 nm; Figure 2) derivatives are typical of globins. Examination of the optical spectrum of the ligand-free ferrous form at pH 7.5 (λ_{max} = 430 and 559 nm; Figure 2) indicates the presence of a five-coordinate high-spin heme.

Temporal Expression Pattern of HbO. As a first step in revealing the physiological function of HbO, we examined the temporal expression pattern of HbO in *M. bovis* BCG ATCC 35734, the nonpathogenic model for *M. tuberculosis*. In this study, polyclonal antibodies raised against HbO were used to detect the presence of this polypeptide in Western blot analysis. As shown in Figure 3, in aerobic cultures, near-steady levels of HbO are detected throughout the growth phase. This is in sharp contrast to that observed for HbN, which is only detected after cells have reached the stationary phase (Figure 3, insets).

Resonance Raman Spectra of the Ferric and Ferrous Protein. On the basis of resonance Raman data, the deoxy form of HbO has a typical five-coordinate high-spin heme, which is consistent with the observation from optical absorption measurements. The frequency of the Fe−His stretching mode was identified at 226 cm^{-1} (*33*), confirming the prediction from the sequence alignment that His is the proximal ligand. This frequency is the same as that in HbN and is significantly higher than that in mammalian hemoglobins (Table 1), suggesting that there is no or little proximal strain in these two hemoglobins. To infer functional properties of HbO, in the work presented here, we examined the liganded forms of the wild type, the B10 Tyr → Phe mutant of HbO, and the CD1 Tyr → Phe mutant of HbO.

CO-Bound Ferrous Protein. In the resonance Raman spectrum of the wild-type CO-bound ferrous protein, a line was detected at 525 cm^{-1} with $^{12}C^{16}O$ and was shifted to 513 cm^{-1} with $^{13}C^{18}O$. It is assigned as the Fe−CO stretching mode (Figure 4a). In the C−O stretching frequency region of the wild-type protein, a line was detected at 1914 cm^{-1} in the $^{12}C^{16}O$ derivative and was shifted to 1828 cm^{-1} with $^{13}C^{18}O$ (Figure 4b). Because of the electronic structure of the Fe−C−O moiety, when the distal interactions strengthen the C−O bond, the Fe−CO bond is weakened concomitantly (or vice versa). As a consequence, there is an inverse correlation curve relating the frequencies of the Fe−CO stretching modes with those of the associated C−O stretching modes (*34*−*36*). These curves depend on the identity of the proximal ligand, such that the curve for imidazole/histidine

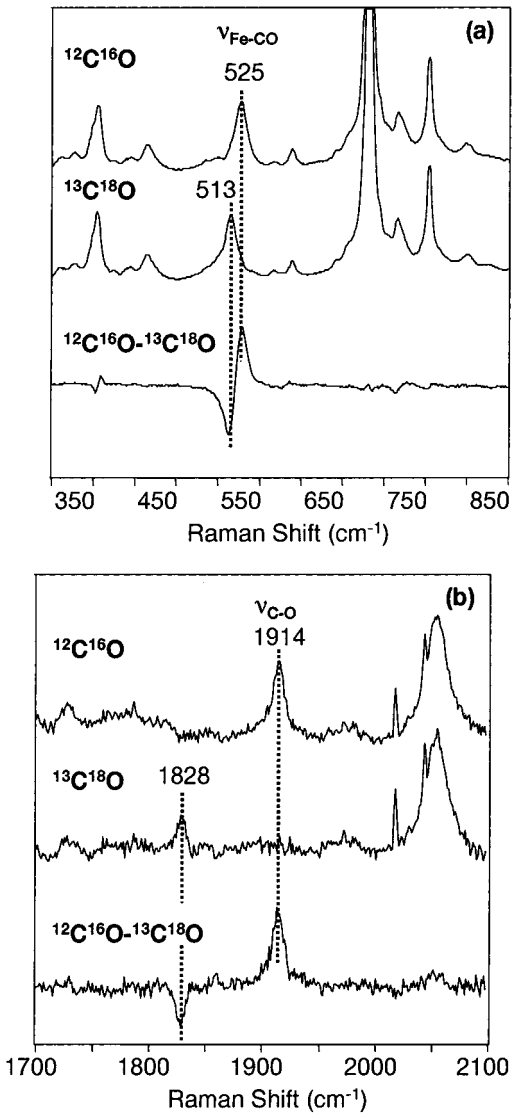

FIGURE 4: Raman spectra of $^{12}C^{16}O$- and $^{13}C^{18}O$-coordinated forms of HbO in pH 7.5 Tris buffer, and the difference spectrum between them in the low-frequency (a) and high-frequency regions (b).

is distinct from that of thiolate. Like other globins, the correlation between ν_{C-O} and ν_{Fe-CO} for HbO falls on the His correlation curve (Figure 5), which further confirms that the proximal ligand is His.

When the B10 Tyr or the CD1 Tyr was mutated to Phe, the Fe−His stretching mode in the ligand-free form was not affected (Table 1), suggesting that this mutation does not perturb the chemical nature of the proximal Fe−His bond. On the other hand, the full width at half-maximum of the Fe−CO stretching mode of the B10 Tyr → Phe mutant increases from 16 to 34 cm^{-1} as compared to that of the wild-type protein, although the frequency of the peak maximum stays constant (Figure 6). In the CD1 Tyr → Phe mutant, the Fe−CO stretching frequency is shifted from 525 to 515 cm^{-1}, suggesting that the mutation in the CD1 Tyr alters the distal pocket structure, which, in turn, modifies the chemical nature of the Fe−CO bond.

Oxygen-Bound Ferrous Protein. In the resonance Raman spectra of the ferrous oxy derivatives of both the wild type and the B10 Tyr → Phe mutant, one Fe−O_2 stretching mode was detected at 559 cm^{-1}, which shifted to ~535 cm^{-1} for $^{18}O_2$ as shown in Figure 7. A surprising feature in both the

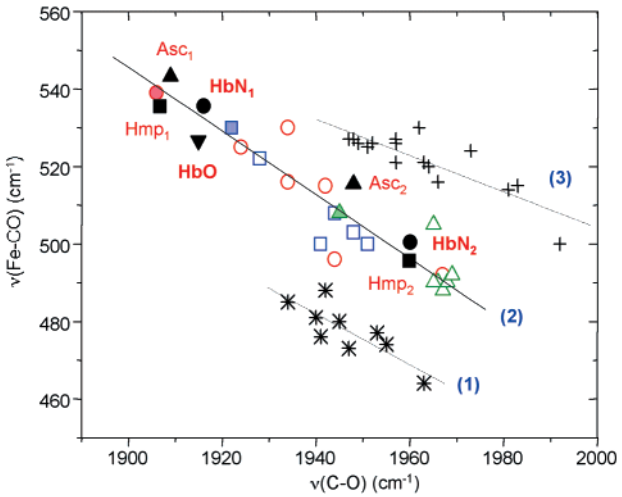

FIGURE 5: Inverse correlation diagram of the Fe−CO stretching frequency vs the C−O stretching frequency of a variety of heme proteins and porphyrin derivatives. Lines 1 and 2 are for complexes in which the proximal ligand is thiolate and histidine, respectively. Line 3 is for five-coordinate CO adducts. The identity of each data point, except HbO, is described in the literature (*29*, *36*, *38*, *47*).

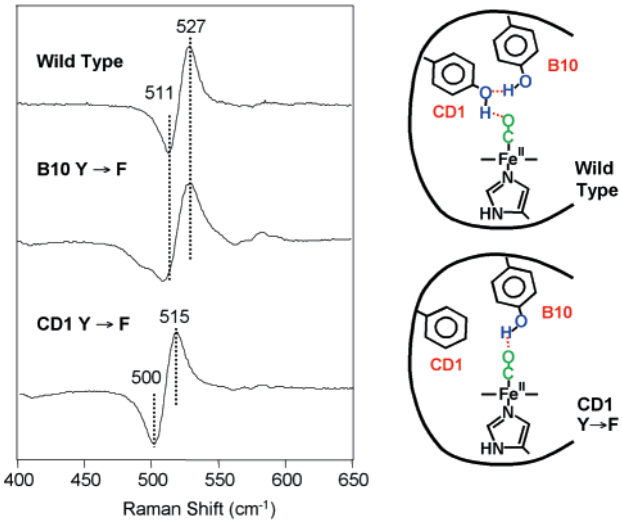

FIGURE 6: (Left) Raman difference spectra ($^{12}C^{16}O$ minus $^{13}C^{18}O$ derivative) of the wild type, the B10 Tyr → Phe mutant of HbO, and the CD1 Tyr → Phe mutant of HbO in pH 7.5 Tris buffer. (Right) Schematic drawing illustrating the interaction between the heme-bound CO and the distal residues.

wild-type protein and the B10 mutant is the presence of the O−O stretching mode (Figure 7). The O−O stretching mode, identified at 1140 cm^{-1}, shifted to 1064 cm^{-1} upon isotope substitution with $^{18}O_2$. This mode is rarely observed in the Raman spectra of globins containing an iron heme (*37*). The presence of the O−O stretching mode in the spectrum of HbO suggests that the distal heme pocket of HbO is atypical among the globin family. The low frequency of this mode, as compared to 1556 cm^{-1} for molecular oxygen, indicates that the heme-bound dioxygen has superoxide character as concluded for many other globins (*37*). When the CD1 Tyr of HbO is mutated to Phe, the Fe−O_2 stretching frequency shifted down slightly from 559 to 556 cm^{-1} and the O−O stretching mode disappeared. The disappearance of the O−O stretching mode suggests that the unique distal pocket structure of HbO is radically altered by this mutation.

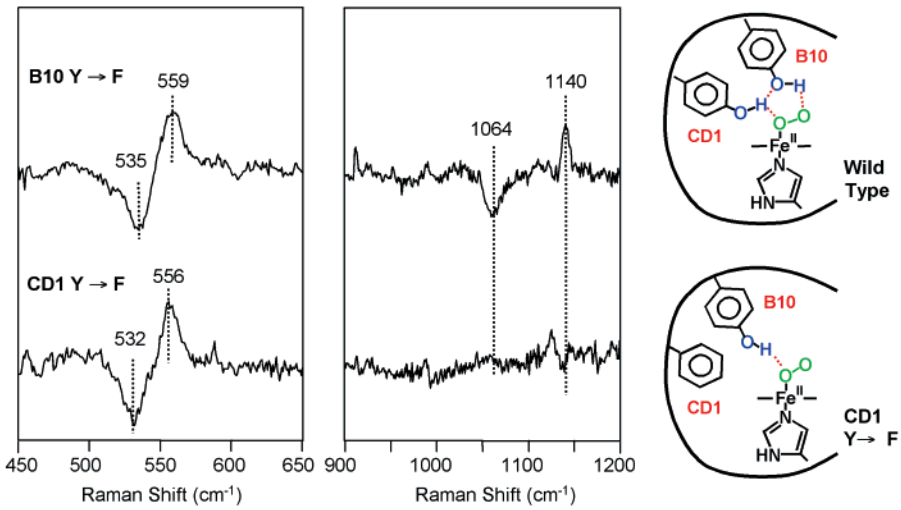

FIGURE 7: (Left) Raman difference spectra ($^{16}O_2$ minus $^{18}O_2$ derivative) of the B10 Tyr → Phe mutant and the CD1 Tyr → Phe mutant of HbO in pH 7.5 Tris buffer. (Right) Schematic drawing illustrating the interaction between the heme-bound O_2 and the distal residues.

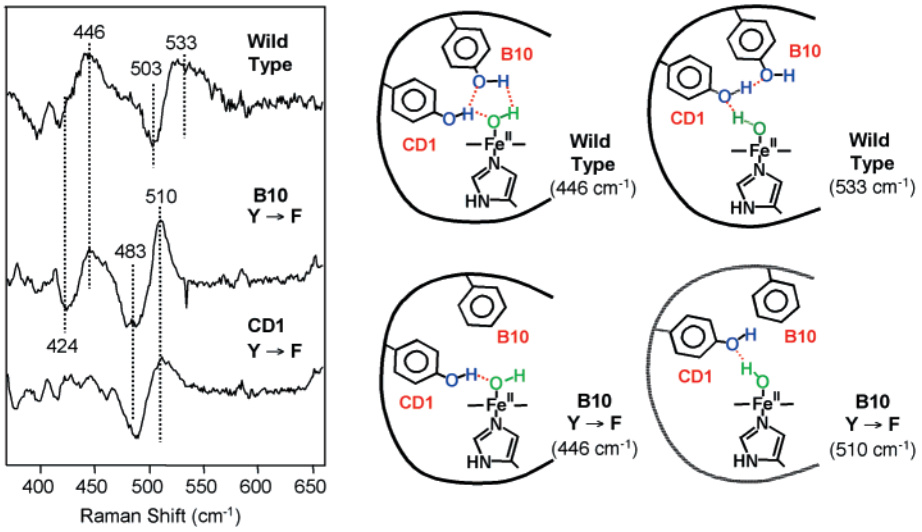

FIGURE 8: (Left) Raman difference spectra ($^{16}OH^-$ minus $^{18}OH^-$ derivative) of the wild type, the B10 Tyr → Phe mutant of HbO, and the CD1 Tyr → Phe mutant of HbO in pH 10.5 CAPS buffer. (Right) Schematic drawing illustrating the interaction between the heme-bound OH^- and the distal residues.

Hydroxide-Bound Ferric Protein. At neutral pH, the resonance Raman spectrum of the ferric protein is primarily six-coordinate and high-spin as indicated by the 1480 and 1563 cm^{-1} lines for ν_3 and ν_2, respectively (data not shown). A contribution from a six-coordinate low-spin form developed as the pH was increased from 7.5 to 10.5 as indicated by an increase in the intensity of the lines at 1506 and 1583 cm^{-1} for ν_3 and ν_2, respectively (data not shown). With $H_2{}^{16}O$ and $H_2{}^{18}O$ isotopic substitution at pH 10.5, two isotope sensitive lines were detected at 446 and 533 cm^{-1} (Figure 8). These two vibrational modes are assigned as the Fe−OH^- stretching frequencies of six-coordinate high-spin and low-spin species, respectively. The doublet in the negative peak of the high-spin species in the isotope difference spectrum is attributed to Fermi resonance coupling of this mode to other porphyrin modes. In the spectrum of the B10 Tyr → Phe mutant, although the 446 cm^{-1} mode stayed unchanged, to our surprise, the 533 cm^{-1} mode shifted to 510 cm^{-1} (Figure 8). On the other hand, in the spectrum of the CD1 Tyr → Phe mutant, the 446 cm^{-1} mode disappeared and the 533 cm^{-1} mode shifted to 510 cm^{-1}, the same position as that observed in the B10 Tyr → Phe mutant (Figure 8). These results indicate that both the B10 and CD1 Tyr play important roles in interacting with the heme-bound hydroxide.

DISCUSSION

Role of the B10 and CD1 Tyr. The Fe−CO stretching mode of HbO observed at 525 cm^{-1} is higher than that in most globins (Table 1). It is well established that positive polar interactions weaken the C−O bond (lowering its stretching frequency) and concurrently strengthen the Fe−CO bond (increasing its stretching frequency) (*29*, *34*−*36*). This is illustrated in Figure 5 by the well-known correlation curve between ν_{Fe-CO} and ν_{C-O}. In this correlation diagram, HbO is located in the top left corner of the curve, which consists of a cluster of other globins with positive polar distal environments (*38*). Consequently, the CO form of HbO is assigned as a closed conformation in which the heme-bound CO strongly interacts with the distal polar residues. Mutation of the B10 Tyr to Phe does not affect the Fe−CO stretching frequency, but it causes broadening of the peak. It suggests that the distal environment of the heme-bound CO in the mutant protein is comparable to that of the wild-type protein;

however, the conformational freedom of the heme-bound CO is considerably increased. On the other hand, mutation of the CD1 Tyr to Phe causes the Fe−CO stretching frequency to shift down to 515 cm^{-1}, which is still ∼15−25 cm^{-1} higher than that of a fully opened distal pocket (Table 1).

Taken together, these observations indicate that in the wild-type protein the CD1 Tyr is interacting with the heme-bound CO, presumably through a hydrogen bond to the oxygen atom of CO. Furthermore, we postulate that the CD1 Tyr also forms a hydrogen bond with the B10 Tyr as illustrated by the top cartoon in Figure 6. In the absence of this hydrogen bond, the protein loses its rigidity as reflected by the increase in the conformational freedom of the Fe−CO bond in the B10 Y → F mutant. In the absence of the CD1 Tyr, the B10 Tyr can interact with the heme-bound CO through a relatively less favorable hydrogen bonding interaction as indicated by the shift of the Fe−CO stretching frequency to a lower value (515 cm^{-1}). This hydrogen bonding interaction is illustrated by the bottom cartoon in Figure 6.

The Fe−O_2 stretching mode of HbO, observed at 559 cm^{-1}, is ∼10 cm^{-1} lower than the typical frequency observed for most mammalian globins (*39*−*42*). This frequency is unaffected by the B10 Y → F mutation, and was slightly downshifted to 556 cm^{-1} upon introduction of the CD1 Y → F mutation. It has been demonstrated that the Fe−O_2 stretching frequency of globins is relatively insensitive to the presence of the hydrogen bonding to the *terminal* oxygen of the heme-bound dioxygen (*29*, *39*). Previously, we have shown that hydrogen bonding to the *proximal* atom of the heme-bound O_2 causes a significant lowering of the Fe−O_2 stretching frequency (*29*, *37*). Thus, the low frequency of this mode in the wild type and the B10 mutant of HbO suggests that the proximal oxygen atom of the heme-bound dioxygen forms a hydrogen bond with the CD1 Tyr residue in both the wild-type and the B10 mutant protein. This is consistent with the observation that mutation of the Tyr at the B10 position to Phe results in only a minor decrease in oxygen affinity (M. Guertin et al., unpublished results), in sharp contrast to the findings with *M. tuberculosis* HbN and *Chlamydomonas* trHb (*12*, *28*), in which the heme-bound oxygen is mainly stabilized by the B10 Tyr. If the hydrogen bond between the CD1 and the B10 Tyr is present in the oxy derivative of the wild-type protein, like that in the CO derivative, it is plausible that the terminal oxygen of the heme-bound dioxygen also forms a H-bond with the B10 Tyr due to their spatial proximity and the stabilization energy gained by forming a five-membered ring structure as illustrated in the top cartoon of Figure 7. To evaluate the feasibility of this proposal, we examined the crystal structure of the trHb from *Chlamydomonas eugametos*. In this structure, the para carbon of the CD1 Phe is pointing toward the heme iron and the linear distance between this para carbon of the Phe and the heme iron is only ∼5 Å (*4*). If the CD1 Phe is replaced with a Tyr, the OH group of this Tyr ought to be close enough to form a hydrogen bond to the heme-bound dioxygen as illustrated in Figure 9. In addition, on the basis of this postulated structure, the B10 Tyr is also in a favorable position to form a hydrogen bond with the terminal oxygen atom of the heme-bound dioxygen.

In the B10 mutant, the hydrogen bonding network is interrupted. However, the critical interaction between the CD1 Tyr and the proximal oxygen atom of the heme-bound dioxygen persists, and as a result, the Fe−O_2 stretching frequency is unchanged. On the other hand, in the CD1 mutant, this critical H-bond is disrupted and the structure is rearranged. A new and stronger H-bond is formed between the B10 Tyr and the proximal oxygen atom of the heme-bound dioxygen as reflected by a further downshift of the Fe−O_2 stretching frequency to 556 cm^{-1} as illustrated in the bottom cartoon of Figure 7.

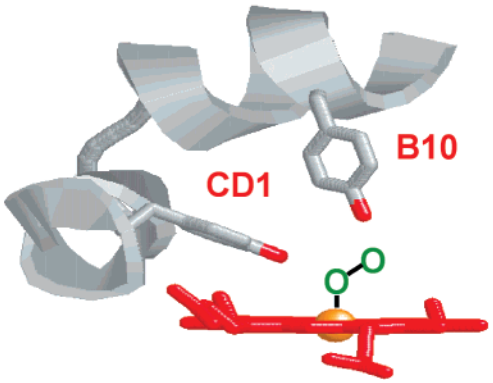

FIGURE 9: Postulated structure of the oxy derivative of HbO based on the structure of *C. eugametos* Hb (PDB entry 1DLY).

The presence of the hydrogen bond between the CD1 Tyr and the proximal oxygen atom of the heme-bound dioxygen forms creates a unique distal heme environment as reflected by the presence of the unusual O−O stretching frequency at ∼1140 cm^{-1}. The O−O stretching mode was not observed in the resonance Raman spectra of any dioxygen-bound globin until recently. It was first detected in the oxy derivatives of the trHbs from *C. eugametos* and *Synechocystis* PCC6803 (*37*). It was proposed that the heme-bound dioxygen is stabilized by a H-bonding network involving both oxygen atoms of the dioxygen, a Tyr at the B10 position, and a Gln at the E7 position, and the enhancement of the O−O stretching mode is due to this H-bonding network. The presence of this O−O stretching mode in the wild type and the B10 Tyr → Phe mutant of HbO and the absence of this mode in the CD1 Tyr → Phe mutant suggest that the presence of this mode in HbO is due to the presence of H-bonding between the dioxygen and the Tyr at the CD1 position, and it is not associated with the H-bonding interaction with the Tyr at the B10 position.

In the hydroxide-bound ferric protein, the Fe−OH^- stretching frequencies of the high-spin and low-spin conformations were observed at 446 and 533 cm^{-1}, respectively (Table 1). The high-spin mode at 446 cm^{-1} is assigned to a conformation in which the oxygen atom of the heme-bound hydroxide forms a hydrogen bond with the CD1 Tyr as illustrated in the right panel of Figure 8. In this model, it is assumed that the hydrogen bond between the B10 Tyr and the CD1 Tyr is present in the ferric protein, like that in the O_2 and CO derivatives. The hydrogen bond between the CD1 Tyr and the oxygen atom of the heme-bound hydroxide withdraws electron density away from the hydroxide, which, in turn, makes it a weak field ligand conferring a high-spin electronic configuration to the heme iron. This scenario is consistent with the observation that this mode was not affected by the B10 Tyr mutation, and it disappeared when the CD1 Tyr was mutated to Phe.

The low-spin mode at 533 cm^{-1}, on the other hand, is assigned to a conformation in which the hydrogen atom of the heme-bound hydroxide forms a hydrogen bond with either the CD1 or B10 Tyr residue (one of the two conformations is illustrated in Figure 8). In the B10 mutant, the loss of the hydrogen bond between the CD1 Tyr and the B10 Tyr relaxes the structural constraint, and as a result, a stronger hydrogen bond is formed between the CD1 Tyr and the heme-bound hydroxide as illustrated in Figure 8 (likewise for the CD1 mutant). The new hydrogen bond makes the hydroxide a weaker ligand and results in a lower $Fe-OH^-$ stretching frequency (510 cm^{-1}). It should be noted that a low $Fe-OH^-$ stretching mode has also been observed at 503 cm^{-1} for the low-spin species of horseradish peroxidase (HRP). It is ~50 cm^{-1} lower than that in most globins (Table 1). It is believed that a strong hydrogen bond between the heme-bound hydroxide and the distal His42 and/or Arg38 is responsible for this weak $Fe-OH^-$ bond in HRP (*40*).

Functional Implications. Recent experiments showing that invertebrate and bacterial hemoglobins protect cells from damage by ambient NO or O_2 through NO/oxygen chemistry (*3*, *5*, *28*, *38*, *43*−*45*) have challenged our perception that globins are generally involved in oxygen transport. This has led to the proposal that ancient hemoglobin is an enzyme that uses redox chemistry to battle against toxic NO or O_2 molecules, and it is later on during evolution that its role transformed into O_2 delivery as seen at present in animals. In parallel with these findings, we have proposed that one of the physiological functions of HbN is to scavenge NO (*28*, *29*). In the study presented here, we have demonstrated that the unique hydrogen bonding network composed of the CD1 Tyr, the B10 Tyr, and the heme-bound ligands in HbO, as illustrated in Figures 6−8, creates a rigid and crowded distal pocket, which is distinct from that of HbN (*29*). It suggests that the physiological roles of HbN and HbO may be quite different, and the unusual role played by the CD1 Tyr in HbO may be crucial for it to perform its physiological functions. The presence of Tyr in the CD1 position of a group of trHbs from high-GC, Gram-positive bacteria, including *M. tuberculosis*, *M. avium*, *M. leprae*, *C. diphterae*, and *S. coelicolor* (Figure 1), supports a unique functional role for CD1 Tyr. Substitution of the highly conserved CD1 Phe for Tyr may represent an ancient and selective adaptation for function in this group of bacteria. Although the extent of amino acid identity between HbO and HbN is low (~18%), the level of identity between HbO and those globins from *M. avium* (84%), *M. leprae* (83%), *C. diphterae* (64%), and *S. coelicolor* (66%) is much higher. Likewise, HbN overall is 79% identical with its orthologue in *M. avium*. These observations all support the proposal that HbO belongs to a distinct group in the trHb family that contains a Tyr at the CD1 position (*21*). In agreement with this concept, physiological studies performed with *M. bovis* BCG demonstrate that the expression of HbN is greatly enhanced during the stationary phase in aerobic cultures, in contrast to the steady expression of HbO throughout the growth curve (Figure 3). The differences in the temporal expression pattern of HbN and HbO in the BCG cells further support the hypothesis that these two hemoglobins may perform very different physiological functions. Additional approaches, such as creation of *M. tuberculosis* strains harboring inactivated *glbN* and *glbO* genes, and quantitative evaluation of the activity of oxy-HbN and oxy-HbO toward NO, are now required to help clarify their roles and are underway in our laboratory.

ACKNOWLEDGMENT

We thank Dr. Denis L. Rousseau for many valuable discussions.

REFERENCES

1. Hardison, R. (1998) *J. Exp. Biol. 201*, 1099−1117.
2. Imai, K. (1999) *Nature 401*, 437, 439.
3. Minning, D. M., Gow, A. J., Bonaventura, J., Braun, R., Dewhirst, M., Goldberg, D. E., and Stamler, J. S. (1999) *Nature 401*, 497−502.
4. Pesce, A., Couture, M., Dewilde, S., Guertin, M., Yamauchi, K., Ascenzi, P., Moens, L., and Bolognesi, M. (2000) *EMBO J. 19*, 2424−2434.
5. Poole, R. K., and Hughes, M. N. (2000) *Mol. Microbiol. 36*, 775−783.
6. Bolognesi, M., Bordo, D., Rizzi, M., Tarricone, C., and Ascenzi, P. (1997) *Prog. Biophys. Mol. Biol. 68*, 29−68.
7. Kapp, O. H., Moens, L., Vanfleteren, J., Trotman, C. N., Suzuki, T., and Vinogradov, S. N. (1995) *Protein Sci. 4*, 2179−2190.
8. Iwaasa, H., Takagi, T., and Shikama, K. (1989) *J. Mol. Biol. 208*, 355−358.
9. Potts, M., Angeloni, S. V., Ebel, R. E., and Bassam, D. (1992) *Science 256*, 1690−1691.
10. Takagi, T., Iwaasa, H., Yuasa, H., Shikama, K., Takemasa, T., and Watanabe, Y. (1993) *Biochim. Biophys. Acta 1173*, 75−78.
11. Couture, M., Chamberland, H., St-Pierre, B., Lafontaine, J., and Guertin, M. (1994) *Mol. Gen. Genet. 243*, 185−197.
12. Couture, M., Das, T. K., Lee, H. C., Peisach, J., Rousseau, D. L., Wittenberg, B. A., Wittenberg, J. B., and Guertin, M. (1999) *J. Biol. Chem. 274*, 6898−6910.
13. Vasudevan, S. G., Armarego, W. L., Shaw, D. C., Lilley, P. E., Dixon, N. E., and Poole, R. K. (1991) *Mol. Gen. Genet. 226*, 49−58.
14. Ermler, U., Siddiqui, R. A., Cramm, R., and Friedrich, B. (1995) *EMBO J. 14*, 6067−6077.
15. Iwaasa, H., Takagi, T., and Shikama, K. (1992) *J. Mol. Biol. 227*, 948−954.
16. Cramm, R., Siddiqui, R. A., and Friedrich, B. (1994) *J. Biol. Chem. 269*, 7349−7354.
17. Zhu, H., and Riggs, A. F. (1992) *Proc. Natl. Acad. Sci. U.S.A. 89*, 5015−5019.
18. Tarricone, C., Galizzi, A., Coda, A., Ascenzi, P., and Bolognesi, M. (1997) *Structure 5*, 497−507.
19. Bolognesi, M., Boffi, A., Coletta, M., Mozzarelli, A., Pesce, A., Tarricone, C., and Ascenzi, P. (1999) *J. Mol. Biol. 291*, 637−650.
20. Milani, M., Pesce, A., Ouellet, Y., Ascenzi, P., Guertin, M., and Bolognesi, M. (2001) *EMBO J. 20*, 3902−3909.
21. Wittenberg, J. B., Bolognesi, M., Wittenberg, B. A., and Guertin, M. (2001) *J. Biol. Chem. 5*, 5.
22. Cole, S. T., Brosch, R., Parkhill, J., Garnier, T., Churcher, C., Harris, D., Gordon, S. V., Eiglmeier, K., Gas, S., Barry, C. E., III, Tekaia, F., Badcock, K., Basham, D., Brown, D., Chillingworth, T., Connor, R., Davies, R., Devlin, K., Feltwell, T., Gentles, S., Hamlin, N., Holroyd, S., Hornsby, T., Jagels, K., Barrell, B. G., et al. (1998) *Nature 393*, 537−544.
23. Olson, J. S., Eich, R. F., Smith, L. P., Warren, J. J., and Knowles, B. C. (1997) *Artif. Cells, Blood Substitutes, Immobilization Biotechnol. 25*, 227−241.
24. Olson, J. S., Mathews, A. J., Rohlfs, R. J., Springer, B. A., Egeberg, K. D., Sligar, S. G., Tame, J., Renaud, J. P., and Nagai, K. (1988) *Nature 336*, 265−266.
25. Yang, J., Kloek, A. P., Goldberg, D. E., and Mathews, F. S. (1995) *Proc. Natl. Acad. Sci. U.S.A. 92*, 4224−4228.

26. Peterson, E. S., Huang, S., Wang, J., Miller, L. M., Vidugiris, G., Kloek, A. P., Goldberg, D. E., Chance, M. R., Wittenberg, J. B., and Friedman, J. M. (1997) *Biochemistry 36*, 13110−13121.
27. Antonini, E., and Brunori, M. (1971) in *Hemoglobin and myoglobin in their reactions with ligands*, pp 70, Elsevier North-Holland, Amsterdam.
28. Couture, M., Yeh, S. R., Wittenberg, B. A., Wittenberg, J. B., Ouellet, Y., Rousseau, D. L., and Guertin, M. (1999) *Proc. Natl. Acad. Sci. U.S.A. 96*, 11223−11228.
29. Yeh, S. R., Couture, M., Ouellet, Y., Guertin, M., and Rousseau, D. L. (2000) *J. Biol. Chem. 275*, 1679−1684.
30. Wheeler, D., Hope, R., Cooper, S. B., Dolman, G., Webb, G. C., Bottema, C. D., Gooley, A. A., Goodman, M., and Holland, R. A. (2001) *Proc. Natl. Acad. Sci. U.S.A. 98*, 1101−1106.
31. Wagner, A. (2001) *Trends Genet. 17*, 237−239.
32. Appleby, C. A. (1978) *Methods Enzymol. 52*, 157−166.
33. Savard, P. Y., Yeh, S.-R., Hugues Ouellet, H., and Guertin, M. (2001) (manuscript in preparation).
34. Li, X. Y., and Spiro, T. G. (1988) *J. Am. Chem. Soc. 110*, 6024−6033.
35. Ray, G. B., Li, X.-Y., Ibers, J. A., Sessler, J. L., and Spiro, T. G. (1994) *J. Am. Chem. Soc. 116*, 162−176.
36. Vogel, K. M., Kozlowski, P. M., Zgierski, M. Z., and Spiro, T. G. (2000) *Inorg. Chim. Acta 297*, 11−17.
37. Das, T. K., Couture, M., Ouellet, Y., Guertin, M., and Rousseau, D. L. (2001) *Proc. Natl. Acad. Sci. U.S.A. 98*, 479−484.
38. Mukai, M., Mills, C. E., Poole, R. K., and Yeh, S. R. (2001) *J. Biol. Chem. 276*, 7272−7277.
39. Hirota, S., Li, T., Phillips, G. N., Olson, J. S., Mukai, M., and Kitagawa, T. (1996) *J. Am. Chem. Soc. 118*, 7845−7846.
40. Feis, A., Marzocchi, M. P., Paoli, M., and Smulevich, G. (1994) *Biochemistry 33*, 4577−4583.
41. Song, S., Boffi, A., Chiancone, E., and Rousseau, D. L. (1993) *Biochemistry 32*, 6330−6336.
42. Van Wart, H. E., and Zimmer, J. (1985) *J. Biol. Chem. 260*, 8372−8377.
43. Gardner, P. R., Gardner, A. M., Martin, L. A., and Salzman, A. L. (1998) *Proc. Natl. Acad. Sci. U.S.A. 95*, 10378−10383.
44. Crawford, M. J., and Goldberg, D. E. (1998) *J. Biol. Chem. 273*, 12543−12547.
45. Liu, L., Zeng, M., Hausladen, A., Heitman, J., and Stamler, J. S. (2000) *Proc. Natl. Acad. Sci. U.S.A. 97*, 4672−4676.
46. Das, T. K., Boffi, A., Chiancone, E., and Rousseau, D. L. (1999) *J. Biol. Chem. 274*, 2916−2919.
47. Das, T. K., Friedman, J. M., Kloek, A. P., Goldberg, D. E., and Rousseau, D. L. (2000) *Biochemistry 39*, 837−842.
48. Das, T. K., Lee, H. C., Duff, S. M., Hill, R. D., Peisach, J., Rousseau, D. L., Wittenberg, B. A., and Wittenberg, J. B. (1999) *J. Biol. Chem. 274*, 4207−4212.
49. Das, T. K., Couture, M., Ouellet, Y., Guertin, M., and Rousseau, D. L. (2001) *Proc. Natl. Acad. Sci. U.S.A. 98*, 479−484.
50. Das, T. K., Weber, R. E., Dewilde, S., Wittenberg, J. B., Wittenberg, B. A., Yamauchi, K., Van Hauwaert, M. L., Moens, L., and Rousseau, D. L. (2000) *Biochemistry 39*, 14330−14340.
51. Couture, M., Das, T. K., Savard, P. Y., Ouellet, Y., Wittenberg, J. B., Wittenberg, B. A., Rousseau, D. L., and Guertin, M. (2000) *Eur. J. Biochem. 267*, 4770−4780.
52. Dasgupta, S., Rousseau, D. L., Anni, H., and Yonetani, T. (1989) *J. Biol. Chem. 264*, 654−662.
53. Feis, A., Rodriguez-Lopez, J. N., Thorneley, R. N. F., and Smulevich, G. (1998) *Biochemistry 37*, 13575−13581.

BI0156409